

Article - Health Science/Pharmacognosy

# Botanical Authentication of “Espinheira-Santa” [*Monteverdia ilicifolia* (Mart. ex Reissek) Biral] Samples by FTIR Spectroscopy Coupled with PCA and Photoacoustic Spectroscopy

**Mylena de França Martins<sup>1</sup>**

<https://orcid.org/0000-0002-1179-8682>

**Marcia Viviane Marcon<sup>2</sup>**

<https://orcid.org/0000-0003-1657-9152>

**Cynthia Maria Schnekenberg Egg<sup>3</sup>**

<https://orcid.org/0000-0002-8812-1952>

**Daniele Toniolo Dias<sup>4</sup>**

<https://orcid.org/0000-0003-0451-3340>

**Jane Manfron<sup>1,2</sup>**

<https://orcid.org/0000-0003-1873-2253>

**Jessica Mendes Nadal<sup>2,3\*</sup>**

<https://orcid.org/0000-0002-2419-2110>

**Paulo Vitor Farago<sup>1,2,3</sup>**

<https://orcid.org/0000-0002-9934-4027>

**Andressa Novatski<sup>1,2</sup>**

<https://orcid.org/0000-0002-8327-6285>

<sup>1</sup>Universidade Estadual de Ponta Grossa, Setor de Ciências Biológicas e da Saúde, Programa de Pós-graduação em Ciências da Saúde, Ponta Grossa, Paraná, Brasil; <sup>2</sup>Universidade Estadual de Ponta Grossa, Departamento de Ciências Farmacêuticas, Programa de Pós-Graduação em Ciências Farmacêuticas, Ponta Grossa, Paraná, Brasil; <sup>3</sup>Universidade Estadual de Ponta Grossa, Departamento de Odontologia, Programa de Pós-Graduação em Odontologia, Ponta Grossa, Paraná, Brasil; <sup>4</sup>Universidade Tecnológica Federal do Paraná, Departamento de Física, Campus Ponta Grossa, Paraná, Brasil.

Editor-in-Chief: Yasmine Mendes Pupo  
Associate Editor: Najeh Maissar Khalil

Received: 09-Jun-2023; Accepted: 18-Jul-2023

\*Correspondence: [jessicabem@hotmail.com](mailto:jessicabem@hotmail.com); Tel.: +55 42 991060889 (J.M.N.)

## HIGHLIGHTS

- *Monteverdia ilicifolia* leaves show several botanical adulterations.
- FTIR spectroscopy provided analytical data about the chemical compounds from *M. ilicifolia* samples.
- FTIR spectroscopy coupled with PCA and photoacoustic spectroscopy can be used as analytical tools for the discrimination of *M. ilicifolia* samples.
- Collected and commercial samples of *M. ilicifolia* were suitable differentiated by photoacoustic spectroscopy.

**Abstract:** *Monteverdia ilicifolia* (Mart. ex Reissek) Biral (basionym: *Maytenus ilicifolia* Mart. ex Reissek) (Celastraceae) is popularly known as holy thorn or “espinheira-santa” in Brazil. This herb is traditionally used for gastric and digestive problems. However, similar species are often used as adulterants. Considering the pharmacological interest and the existence of adulterants, this study was devoted to characterizing *M. ilicifolia* samples by Fourier-transform infrared (FTIR) spectroscopy coupled with principal component analysis (PCA)

and photoacoustic spectroscopy (PAS) by using *Citronella gongonha* (Mart.) R. A. Howard as adulterant sample. Six commercial samples were purchased, and seven collected samples were obtained in the Campos Gerais region. The leaves were then dehydrated and converted to powder. The FTIR spectroscopic assay was carried out and consisted of ten different measurements for each sample with a time interval of seven days between them. The PCA was performed from these spectra. The characterization by FTIR demonstrated the presence of tannins and flavonoids in the studied samples. FTIR spectroscopy coupled with PCA was able to discriminate the commercial and the collected samples of *M. ilicifolia* using three principal components. The photoacoustic spectroscopy resulted in absorption bands centered at ~280, ~380, ~480, and ~630 nm. These bands presented a higher spectral resolution for the collected samples. The commercial samples showed broadening bands, which allowed the differentiation between these two sets of samples. FTIR spectroscopy coupled with PCA, and photoacoustic spectroscopy are alternative tools for the differentiation of *M. ilicifolia* samples.

**Keywords:** adulterants; *Citronella gongonha*; Fourier-transform infrared spectroscopy; holy thorn; principal component analysis; total tannins.

---

## INTRODUCTION

The commercial sector of herbal supplements and medicinal plants has presented a remarkable worldwide growth. However, these herbal medicines must show quality, efficacy, and safety for the final consumers, and a current concern in this area is related to the presence of adulterants [1,2]. Adulteration is defined as an intentional substitution or addition of another/ closely related plant species or foreign substance in a genuine medicinal product, in order to increase the weight, the potency of the product, and/or to decrease its cost [3].

In this context, the species *Monteverdia ilicifolia* (Mart. ex Reissek) Biral (Celastraceae), popularly known as holy thorn, “cancerosa”, and “espinheira-santa” in Brazil, is usually confused with other species that show similar leaves [4]. In addition, *M. ilicifolia* was recently renamed since it was previously classified as *Maytenus ilicifolia* Mart. ex Reissek. The characteristics that separated these genera were the fruit pericarp texture and the aril color, which is red or yellowish in the *Maytenus* genus and white in the *Monteverdia* one [5]. Furthermore, holy thorn is widely used in traditional medicine for gastrointestinal, urinary, and endocrine diseases with an emphasis on gastritis and gastric ulcer problems [6]. Its leaves present tannins and flavonoids as the main natural products [7].

Some species morphologically similar to *M. ilicifolia* and with non-related pharmacological properties have been reported in the literature. *Sorocea bonplandii* (Baill.) W.C.Burger, Lanj. & Wess.Boer. (Moraceae), *Zollernia ilicifolia* (Brongn.) Vogel (Fabaceae), *Jodina rhombifolia* (Hook. & Arn.) Reissek (Santalaceae), and *Citronella gongonha* (Mart.) R.A.Howard (Cardiopteridaceae) are the main adulterants for the medicinal products based on holy thorn [8–9]. These adulterations create a lack of quality, which strongly impacts on the efficacy and safety of the medicinal use [10].

Among the recommended techniques for characterizing plant species, the Fourier-transform infrared (FTIR) spectroscopy can be readily used to identify the chemical groups of herbal samples [11] and is considered a fast, low cost, and small sampling method [12]. FTIR spectroscopy becomes a suitable strategy for the analysis of herbal raw materials, since previous studies proved its applicability for the species differentiation, the origin discrimination of plant samples [13], the herbal quality control [14], and the herbal adulteration analysis [15]. In addition, FTIR spectroscopy can be coupled with multivariate analysis by principal components (PCA) for providing a cost-effective approach in order to discriminate groups of herbal samples and to investigate their authenticity, since chemical-based analyses are more labor- and time-consuming [16,17]. Considering the photoacoustic spectroscopy, it is a novel and non-destructive analytical approach for herbal products, suitable for samples with high light scattering and absorption as leaves [18]. This method can also identify different polyphenols in powder mixtures and is independent of the solvent use [19].

Taking all these into account, the aim of this paper was to investigate the botanical authentication of commercial and collected samples of *M. ilicifolia* by FTIR spectroscopy coupled with PCA and photoacoustic spectroscopy compared to the adulterant sample of *C. gongonha* in order to allow their differentiation for the quality control of holy thorn-based products.

## MATERIAL AND METHODS

### Plant material

The plant material used was leaves of *Monteverdia ilicifolia* (Mart. ex Reissek) Biral (Celastraceae) and *Citronella gongonha* (Mart.) R.A.Howard (Cardiopteridaceae). The botanical material was divided in six commercial samples and six collected samples of holy thorn. The collected samples were obtained in the Campos Gerais Region, Paraná, Brazil. The sample of *C. gongonha* used as adulterant for holy thorn was also collected in this same area. The exsiccates of *M. ilicifolia* were deposited and registered at the herbarium of the State University of Ponta Grossa (HUPG) under the numbers 22,245; 22,246; 22,248; 22249; 22,151; and 22,153. The *C. gongonha* sample was recognized by comparison with the specimen ICN 113,385 from the herbarium of the Federal University of Rio Grande do Sul (ICN).

### Sample preparation

The collected samples were firstly submitted to a drying process, in which the leaves were removed and taken to the heat treatment in a lab oven (Odontobras, EI-1.6 model, São Paulo, Brazil) at 40°C for 72 hours [20]. All the samples, including the commercial ones, were converted to powder using a Willey type knife mill with a 32-mesh circular sieve (Tecnal, Piracicaba, Brazil). Each sample was stored in hermetically sealed polypropylene bottles and kept away from light and moisture.

### Fourier Transform Infrared Spectroscopy (FTIR)

The 13 powdered samples were analyzed by FTIR spectroscopy [21] as tablets using 4 mg of each sample and 200 mg of KBr (spectroscopic grade, Sigma Aldrich, St. Louis, MO, USA, 2%, w/w) in the Shimadzu spectrometer (model IR Prestige-21, Kyoto, Japan) at 64 scans/min, resolution of 4 cm<sup>-1</sup>, analysis mode of absorbance, in the range of 4000 to 400 cm<sup>-1</sup> [22, 23]. Ten measurements were performed on each sample with a time interval of seven days.

### Principal Component Analysis (PCA)

The FTIR spectra were submitted to the multivariate analysis by principal components (PCA) [24]. For this analysis, the region between 1800-400 cm<sup>-1</sup> (fingerprint) was chosen since it represented the main information about the natural products presented in the *M. ilicifolia* and *C. gongonha* samples. The principal components (PCs) were obtained as a function of the absorption spectra. The differentiation of the organic groups of the samples was performed from these PCs. The components were generated using the Principal Component Analysis for Spectroscopy Application of the Origin Pro software (version 2020) (Origin Lab, Northampton, MA, USA).

### Photoacoustic Spectroscopy (PAS)

The photoacoustic spectroscopy (PAS) homemade setup was used for evaluating the samples. This apparatus consisted of the 1000 W Xenon lamp (66926, Oriel Instruments, Newport Corporation, Franklin, MA, USA) as the light source, monochromator (CornerstoneTM 260 1/4m, Oriel Instruments), mechanical chopper (SR540, Stanford Research Systems, Sunnyvale, CA, USA), lock-in amplifier (SR830, Stanford Research Systems), and microphone (4953, Brüel and Kjaer Instruments, Santo Amaro, Brazil) coupled to a sealed photoacoustic cell for signal detection [25]. Higher order diffractions were eliminated by bandpass filters. The spectral range for UV-Vis was between 225 and 700 nm. The chopper was tuned to different frequencies to modulate the light that impinges the sample. The data acquisition was performed by a personal computer. To correct the source emission intensity in each wavelength, all spectra were normalized with respect to a carbon black sample signal. The data were evaluated using the Origin Pro software (version 2020) (Origin Lab, Northampton, MA, USA).

## RESULTS AND DISCUSSION

### Fourier Transform Infrared Spectroscopy (FTIR)

FTIR spectroscopy was used for elucidation of functional groups presented in the commercial and collected samples of *Monteverdia ilicifolia* (Mart. ex Reissek) Biral (Celastraceae) and *Citronella gongonha* (Mart.) R.A.Howard (Cardiopteridaceae). *C. gongonha* was the adulterant sample. Figure 1 summarizes all the obtained spectra in the absorbance mode. The main absorption bands were observed at 677; 1070; 1233;

1271; 1321; 1522; 1618; and 1732  $\text{cm}^{-1}$ . The fingerprint region between 1800 and 400  $\text{cm}^{-1}$  provided the unique spectral signature of the *M. ilicifolia* and *C. gongonha* samples and was related to the organic and inorganic compounds found on these samples based on their functional groups and structures.

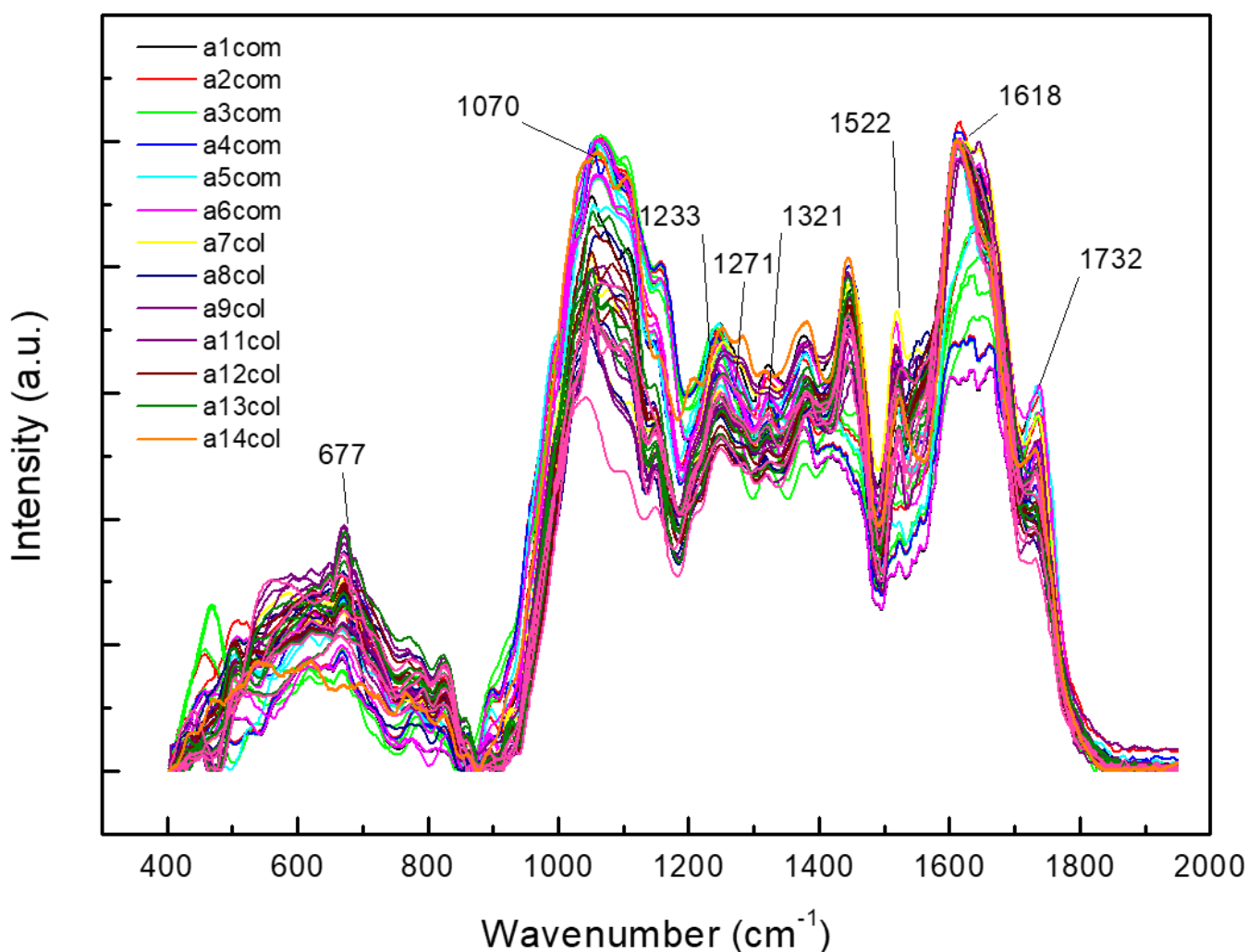


**Figure 1.** FTIR spectra of 12 samples of *Monteverdia ilicifolia* (Mart. ex Reissek) Biral and one adulterant sample of *Citronella gongonha* (Mart.) R.A.Howard. The main bands were achieved at 677; 1070; 1233; 1271; 1321; 1522; 1618; 1732  $\text{cm}^{-1}$ . Abbreviations: com – commercial samples of *M. ilicifolia*; col – collected samples of *M. ilicifolia*; CG – *C. gongonha* sample.

The C=O stretching of esters from hydrolysable tannins was assigned at 1732  $\text{cm}^{-1}$ , mainly those derived from the gallic acid. This region was the principal stretching for differentiating between the condensed and hydrolysable tannins, since the condensed tannins do not present the carboxyl group under natural conditions [26]. Other stretching bands were corresponded to the C=C-C bond from aromatic rings at 1618-1444  $\text{cm}^{-1}$  and the C-O bond at 1368-1157  $\text{cm}^{-1}$  and 1070-1023  $\text{cm}^{-1}$ . In contrast, condensed tannins usually show more intense C=C-C stretching bands when compared to hydrolysable tannins at 1555-1503  $\text{cm}^{-1}$  [26]. However, hydrolysable tannins exhibit more intense C-O stretching signal when compared to condensed tannins at 1368-1157  $\text{cm}^{-1}$ , probably due to the presence of esters. In addition, condensed tannins also show absorptions at 1361-1340  $\text{cm}^{-1}$  and 1284-1283  $\text{cm}^{-1}$ , regions in which absorptions of hydrolysable tannins are not observed. Therefore, these stretching bands were assigned to the C-O bond of pyran rings, typically observed for flavonoids [27–33]. The region between 600-930  $\text{cm}^{-1}$  was attributed to out-of-plane C-H bending of aromatic rings. The signal between 1060-1130  $\text{cm}^{-1}$  was related to in-plane C-H bending of aromatic rings [34–41].

Considering the high number of analytical information and the differences in spectrum intensities obtained by FTIR, we used the principal component analysis for a discriminant analysis about these spectra at the fingerprint region between 400 and 1900  $\text{cm}^{-1}$  [26,42].

## Principal Component Analysis (PCA)

The principal component analysis was performed for the FTIR spectra from 1800 to 400  $\text{cm}^{-1}$  in order to obtain a more accurate result about the differences among the *M. ilicifolia* and *C. gongonha*. All spectra were normalized by the integrated area in the aforementioned region.

The analysis was firstly performed to find out which principal component should be used. The analysis allowed that the data set was visualized concerning the various principal components. The initial set of variables was reduced to a number of principal components, which is represented by the scree plot depicted in Figure 2. This plot provided the inflection point related to the limit of principal components required to represent the examined data.

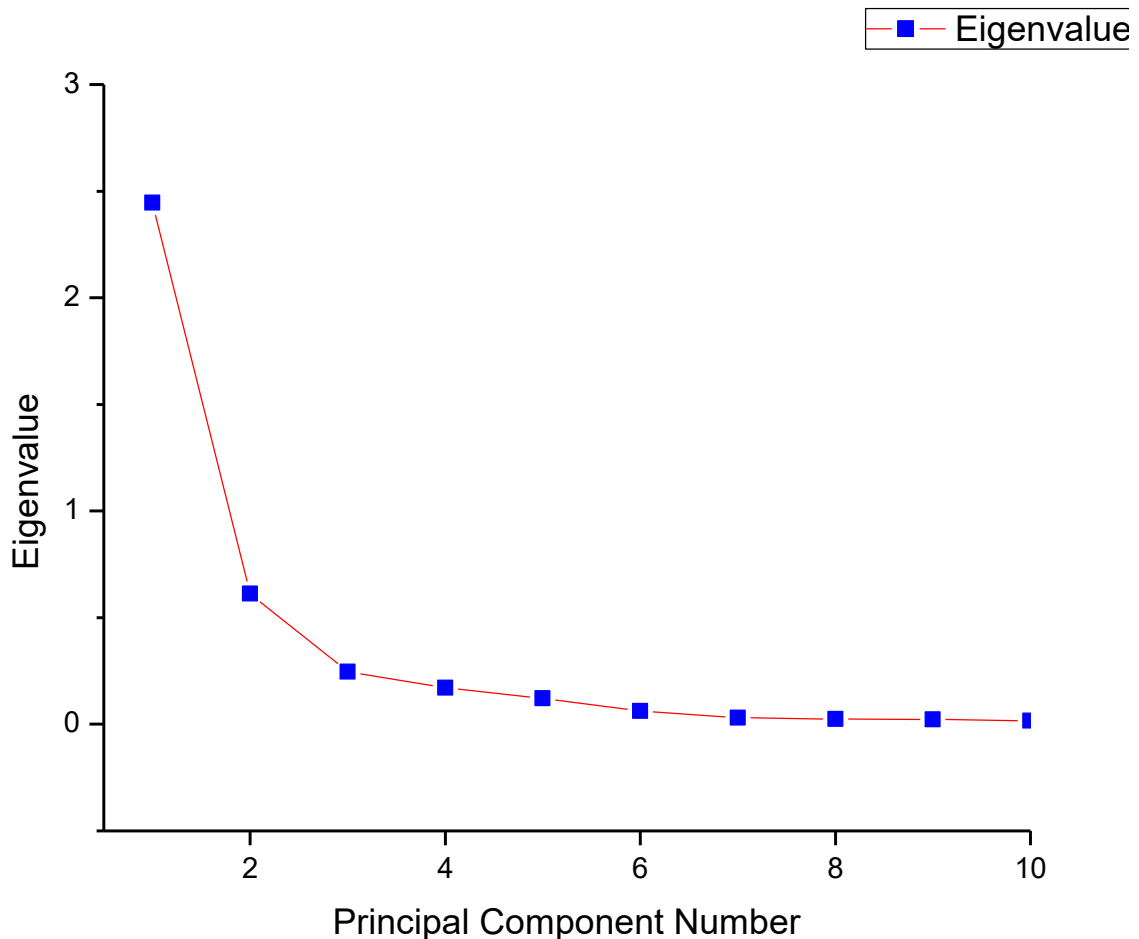


**Figure 2.** Scree plot showing the variance represented by each component from the source eigenvalue. The inflection point determines the limit of components required to represent the analyzed data.

It was observed that the inflexion point was achieved from PC3. In this perspective, PC1 represented 64.3%, PC2 explained 16.1%, and PC3 characterized 6.5% of the analytical data. These values resulted in a total of 86.9% of certainty by reducing the data to three principal components.

Figure 3 shows the PCA scores obtained from the spectra. Figure 3a represents PC1 (64.3%) x PC2 (16.1%), while Figure 3b depicts PC1 (64.3%) x PC3 (6.5%) with the 95% confidence ellipse for each set of samples. PCA was able to provide a separation between commercial and collected samples of *M. ilicifolia*. However, the sample aCG (*C. gongonha*) remained with the commercial samples of holy thorn. The collected samples appeared in positive score for PC1, and positive and negative scores for PC2 and PC3. The commercial samples showed negative score for PC1, and positive and negative scores for PC2 and PC3. The adulterant sample aCG presented negative score for PC1 and positive scores for PC2 and PC3.

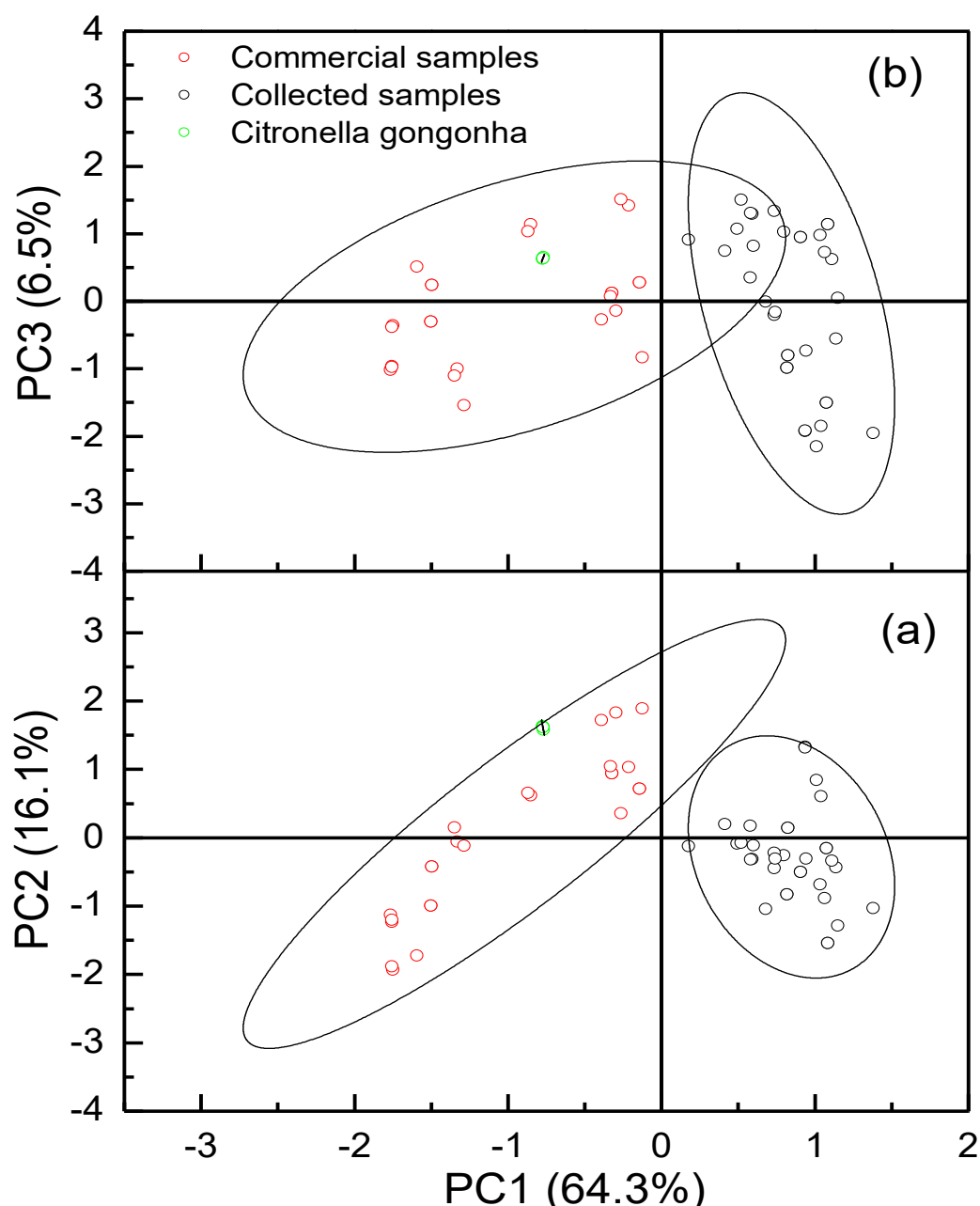


**Figure 3.** PCA scores obtained from the FTIR spectra of the *Monteverdia ilicifolia* (Mart. ex Reissek) Biral and *Citronella gongonha* (Mart.) R.A.Howard samples. The plots represent PC1xPC2 and PC1xPC3. The 95% confidence ellipses are also shown.

In addition to the scores, the loadings provided by PCA added a substantial information. Loadings indicated the weight of the variables (FTIR absorption bands) for each principal component. The loadings for each principal component are summarized in Figure 4. One of the main stretching signals for PC1 analysis was detected at  $1740\text{ cm}^{-1}$ , which can differentiate between hydrolysable and condensed tannins [26]. Considering that the *M. ilicifolia* commercial samples and the adulterant *C. congonha* presented negative loadings, these samples revealed higher concentration of carboxyl groups from hydrolysable tannins.

The region between  $1650$  and  $1380\text{ cm}^{-1}$  had positive loadings. These signals were assigned to the C=C bond stretching of aromatic rings from condensed tannins. These data suggests that the collected samples presented a higher concentration of condensed tannins.

The in-plane bending signal of C-H bonds from aromatic rings, typically detected for hydrolysable tannins, was assigned around  $1100\text{ cm}^{-1}$  as negative loadings and was mainly observed in the *M. ilicifolia* commercial samples. The signals between  $800$ - $700\text{ cm}^{-1}$  were assigned to out-of-plane bending of C-H bonds from aromatic rings in condensed tannins that were mainly presented in collected samples. Therefore, the main absorptions for separating the commercial samples (including aCG) from the collected samples were related to the differentiation between hydrolysable and condensed tannins [26,40].

Two regions showed negative loading at 803 and 893  $\text{cm}^{-1}$  for PC2. These signals corresponded to out-of-plane bending of C-H bonds from aromatic rings, which were naturally found in condensed tannins. In that sense, samples a1com and a2com with negative PC2 scores had the higher concentration of this type of metabolites [34,36]. Among the collected samples, a8col, a12col, and a13col were highlighted with higher concentration of condensed tannins. The band at 444  $\text{cm}^{-1}$  was assigned to the breathing mode from the aromatic ring and also resulted in negative PC2 loadings [37–40].

Negative loadings for PC3 were detected at 1741 and 1703  $\text{cm}^{-1}$ , which corresponded to the C=O stretching. Hence, the samples a3com, a6com, a7col, a9col, a12col, and a13col showed the higher concentration of hydrolysable tannins when compared to the others. The C=C-C stretching revealed positive loadings and was observed at 1448 and 1609  $\text{cm}^{-1}$ . These signals were attributed to condensed tannins. The in-plane bending signal of C-H bonds from aromatic rings was verified at 1100  $\text{cm}^{-1}$  as a positive value, which indicated the discrimination of the samples a1com, a3com, a4com, aCG, a11col, and a8col [29, 35–37,41,43,44].

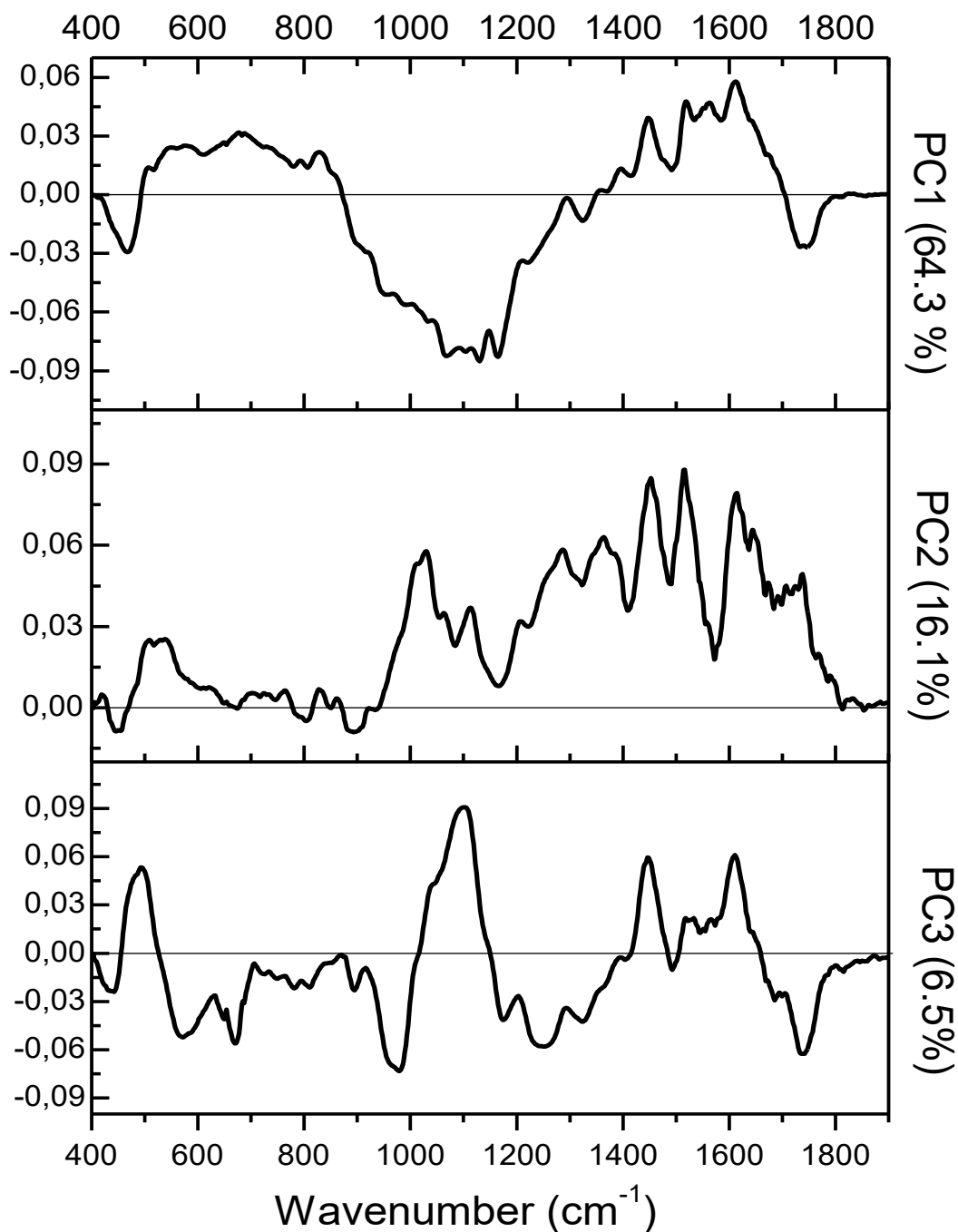


**Figure 4.** PCA loadings obtained for PC1, PC2 and PC3. The three principal components resulted in a total of 86.9% of certainty to explain the analytical data.

## Photoacoustic Spectroscopy (PAS)

The results of photoacoustic spectroscopy are presented in Figure 5. Two bands were observed for the commercial *M. ilicifolia* samples (Figure 5a). The main band was centered at ~280 nm and a broadening signal was observed at ~360 nm. The collected *M. ilicifolia* samples (Figure b) presented more distinct bands at ~280, ~380, ~480, and ~630 nm. The lack of spectral resolution for the commercial samples was also suggestive of the presence of hydrolysable tannins [29].

Gaussian fits were then performed for the spectra of Figure 05, considering the absorption bands set at 280, 380, 480, and 630 nm. Figure 6 shows fitting examples for samples a1com (Figure 6a) and a8col (Figure 6b). In order to compare the Gaussian areas, the position and the width of each absorption center were kept fixed.

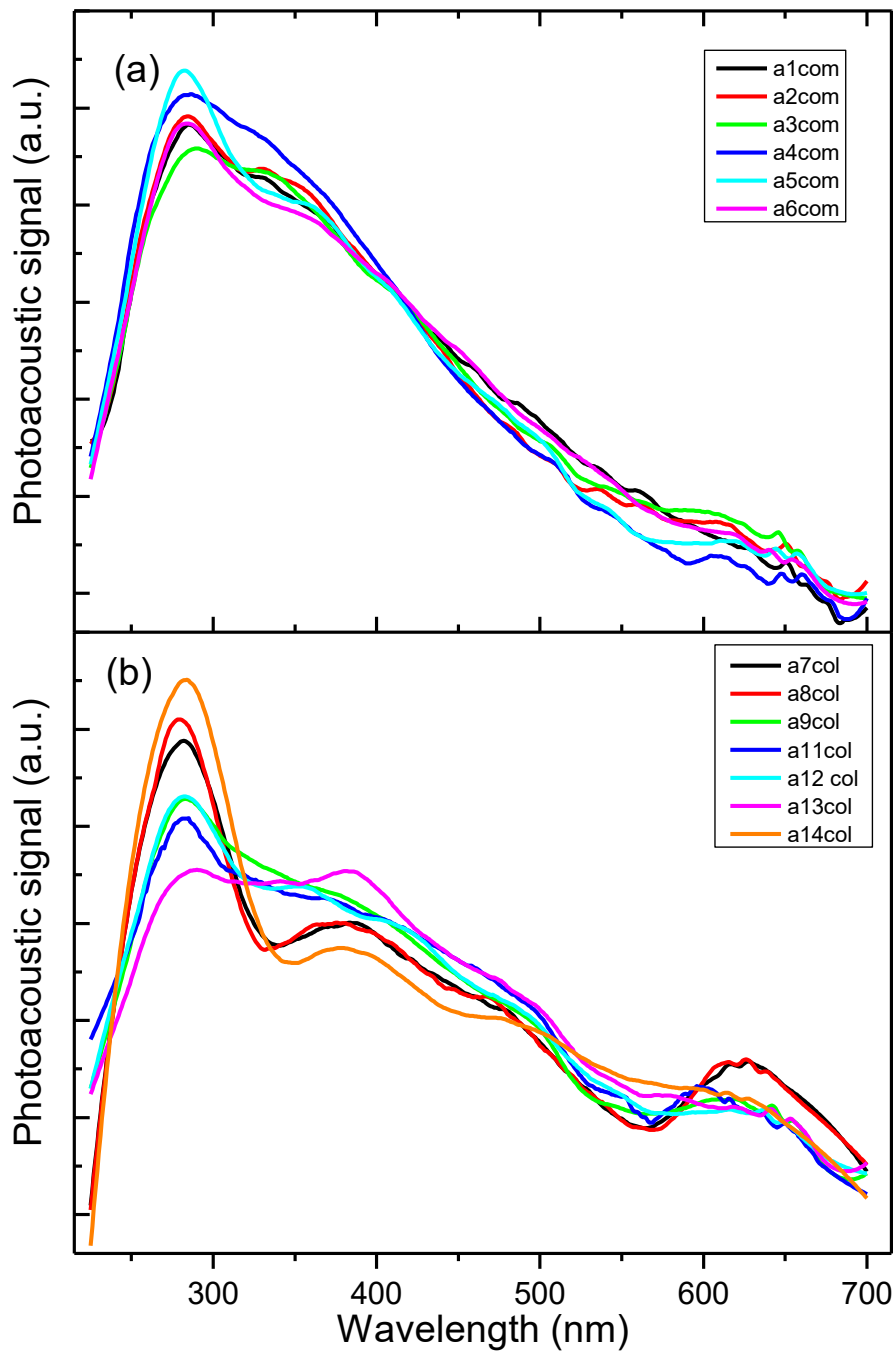


**Figure 5.** Photoacoustic signal for the commercial (a) and collected (b) *M. ilicifolia* samples, including the adulterant sample aCG (b).

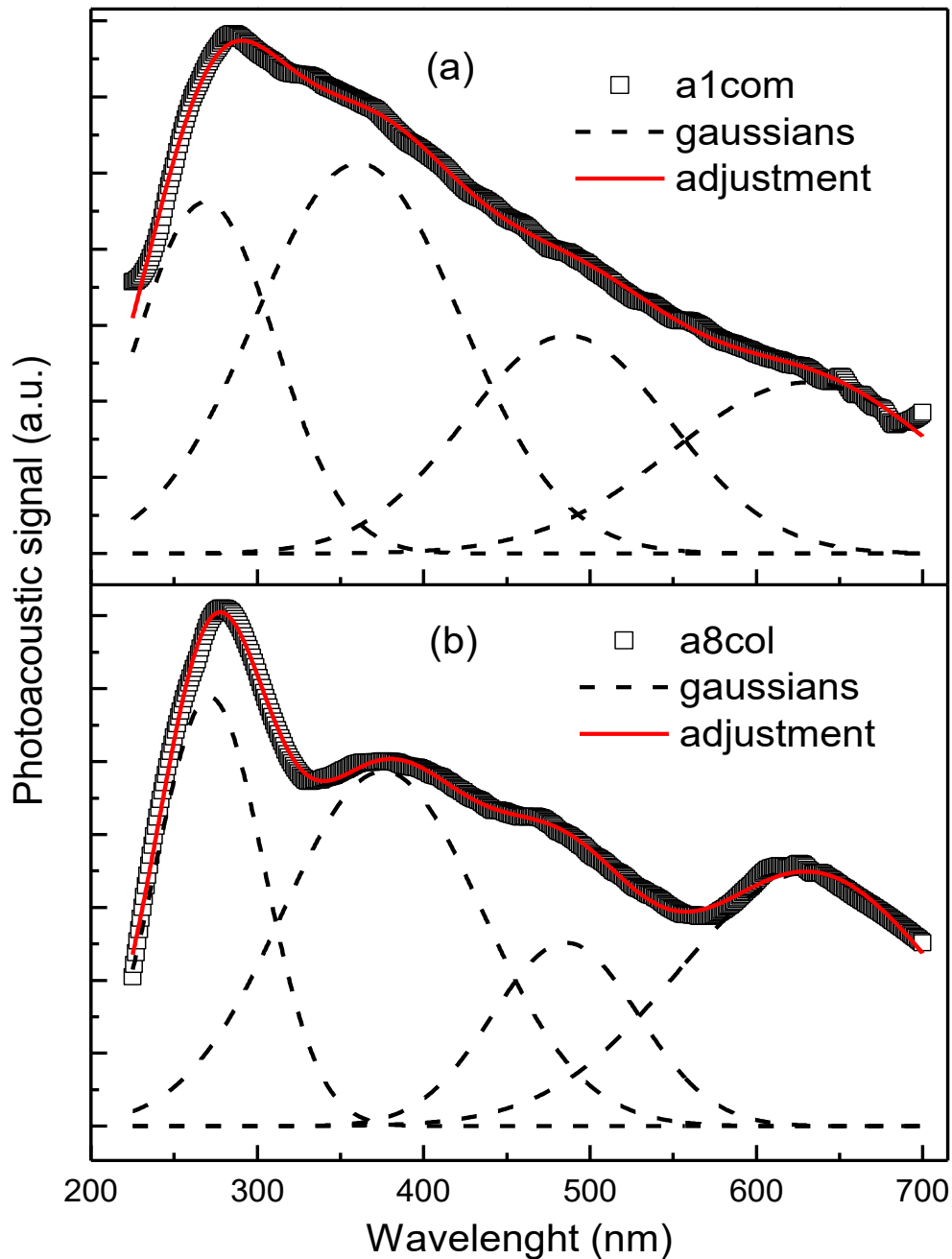


**Figure 6.** Gaussian fits for samples a1com (a) and a8col (b).

Figure 7 summarizes the behavior of the Gaussian areas for the different samples of *M. ilicifolia* and *C. gongonha*. No significant difference was observed for the band area at ~280 nm, excepting the differences for samples a12col, a13col, and aCG, which showed an increase in the band areas. Sample a4com had a broader area at ~380 nm, while samples a12col, a13col, and aCG have a distinct area. The band areas at ~480 and ~630 nm are the ones that separated the commercial *M. ilicifolia* samples from the collected ones. This behavior was highlighted in Figure 7 with pink ellipses. According to Valladão and coauthors, these regions were associated with the absorption of carotenes, chlorophylls, and other similar pigments [45]. Considering these results, different behaviors were observed for the commercial and the collected samples of *M. ilicifolia* by photoacoustic spectroscopy.

This first report about the PAS analysis for the discrimination of *M. ilicifolia* samples paves the way for its use as a feasible analytical tool for the quality control of herbal species. Further analytical studies are required in order to provide a differentiation between *M. ilicifolia* and *C. gongonha* samples.

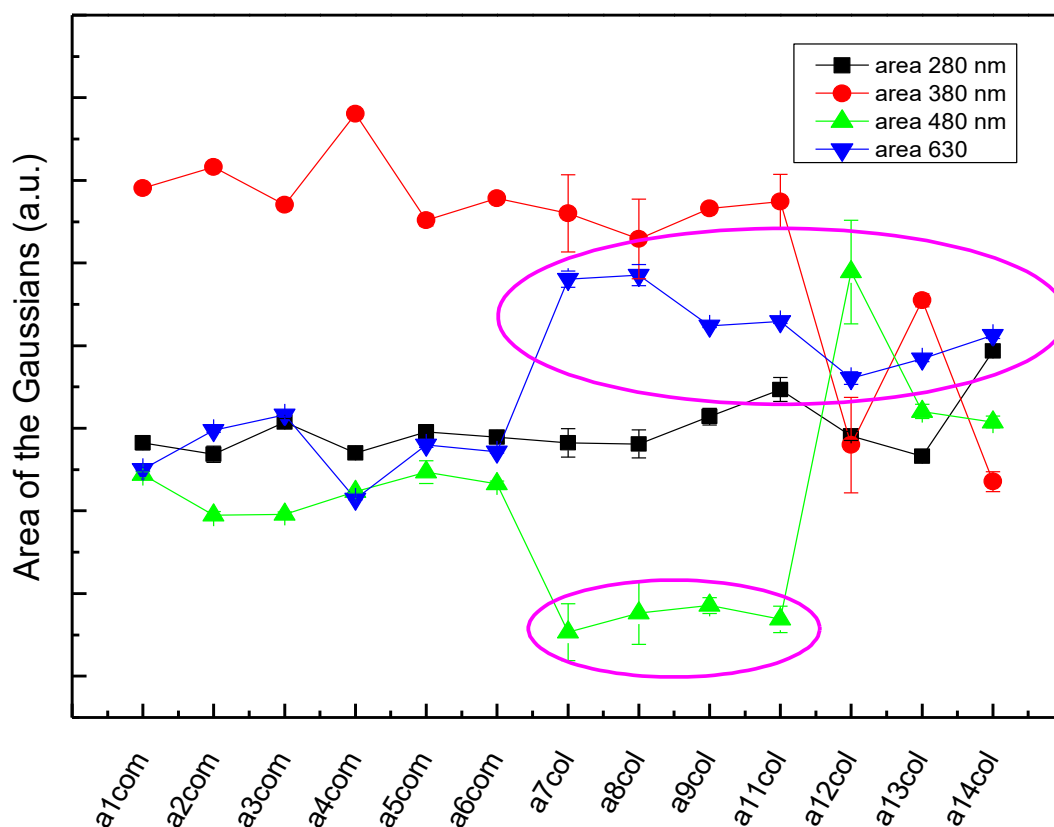


**Figure 7.** Behavior of the Gaussian areas for the commercial and the collected samples of *M. ilicifolia*, and the adulterant sample of *C. gongonha* (aCG).

## CONCLUSION

In this study, the FTIR spectroscopy coupled with PCA and the photoacoustic spectroscopy were used for the botanical authentication of commercial and collected holy thorn or “espinheira-santa” [*Monteverdia ilicifolia* (Mart. ex Reissek) Biral] samples. FTIR spectra revealed the presence of hydrolysable and condensed tannins, and flavonoids in these samples. The FTIR spectroscopy coupled with PCA was able to provide the differentiation between the commercial and the collected samples of *M. ilicifolia*. The photoacoustic spectroscopy after the Gaussian adjustment also allowed the discrimination of *M. ilicifolia* samples and the adulterant *C. gongonha* sample. These analytical methods are feasible alternative tools for the quality control of holy thorn, and can be used for further studies on quality control and adulteration of herbal samples.

**Funding:** This research was funded by CNPq/Brazil, grant numbers 313704/2019-8 and 168149/2022-2.

**Acknowledgments:** The authors are grateful to CLABMU-UEPG for technical support.

**Conflicts of Interest:** The authors declare no conflict of interest.

## REFERENCES

1. Carvalho VAP. [Chemical characterization by liquid chromatography and chemometric analysis of Bauhinia plant species with application in quality control of commercial samples of pata-de-vaca]. [dissertation]. São Carlos (SP): Federal University of São Carlos; 2011. Available: <https://repositorio.ufscar.br/handle/ufscar/6536>
2. Brazil. Ministério da Saúde. Secretariat of Health Care. Department of Basic Care. Ministério da Saúde. Diário da República, 1.a serie. 9. vol, 53, 6297-383.
3. El Beyrouthy M, Abi-Rizk A. DNA fingerprinting: the new trend in fighting the adulteration of commercialized and cultivated medicinal plants. Adv. Crop. Sci. Technol. 2013;1:e107.
4. Yokota AA, Jacomassi E, Laverde Junior A, Takemura OS. Evaluation of the quality of products containing *Maytenus ilicifolia* Mart. ex Reissek - Celastraceae (Espinheira-santa) commercialized in the city of Umuarama – PR. Semina. 2010;31(2):159–68.
5. Biral L, Simmons MP, Smidt EC, Tembrock LR, Bolson M, Archer RH, et al. Systematics of New World *Maytenus* (Celastraceae) and a New Delimitation of the Genus. Syst. Bot. 2017;42(4):1–14. Leonardo Biral, Mark P. Simmons, Eric C. Smidt,

6. Santos-Oliveira R, Coulaud-Cunha S, Colaço W. Review of *Maytenus ilicifolia* Mart. ex Reissek, Celastraceae. Contribution to the studies of pharmacological properties. *Braz. J. Pharmacogn.* 2009;19(2B): 650-9.
7. Jesus WMDM, Cunha TN. Study of the pharmacological properties of espinheira-santa (*Maytenus ilicifolia* Mart. ex Reissek) and two adulterant species. *Rev Saúde e Desenvol.* 2012;1(1):21–46.
8. Ribeiro MV, Almeida C, Oliveira ASC, Vargas NSC, Barbieri RL. Economic reading of the holythorn of the Journey of Post-Graduation and Research in Pelotas, RS. *Congrega Urcamp.* 2016:777–88.
9. Machado AV, Santos M. Comparative leaf morpho-anatomy of species known as espinheira-santa: *Maytenus ilicifolia* (Celastraceae), *Sorocea bonplandii* (Moraceae) and *Zollernia ilicifolia* (Leguminosae). *INSULA J Bot.* 2004; 33:1.
10. Budel JM, Duarte MR, Farago PV, Takeda IJM. [Anatomical characters of leaves and stems from *Calea uniflora* Less., Asteraceae.] *Braz. J. Pharm. Sci.* 2006; 16(30):53-60.
11. Desmarchelier C, Alonso J. *Maytenus ilicifolia* Martius (Congorosa). *Latin American and Caribbean Bulletin of Medicinal Plants and Aromatics*, 2007.
12. Lopes G. [Nafion Membrane Characterization Using Photoacoustic Spectroscopy: Hydration Monitoring.] [dissertação]. Ponta Grossa(PR): Universidade Tecnológica Federal do Paraná; 2016.
13. Kharyuk P, Nazarenko D, Oseledets, I. Comparative study of Discrete Wavelet Transforms and Wavelet Tensor Train decomposition to feature extraction of FTIR data of medicinal plants. *arXiv preprint arXiv:1807.07099*, 2018.
14. Huang Y, Wang L-S, Chao Y-j, Nawawi DS, Akiyama T, Yokoyama T, et al. Analysis of Lignin Aromatic Structure in Wood Fractions Based on IR Spectroscopy. *J. Wood Chem. Technol.* 2016;36(5):377–382.
15. Machado CD, Raman V, Rehman JU, Maia BHLNS, Meneghetti EK. *Schinus molle*: anatomy of leaves and stems, chemical composition and insecticidal activities of volatile oil against bed bug (*Cimex lectularius*)". *Braz. J. Pharmacog.* 2019;29(31):1-10.
16. Budel JM, Wang M, Raman V, Zhao J, Khan SI, Rehman JU, et al. Essential Oils of Five *Baccharis* Species: Investigations on the Chemical Composition and Biological Activities. *Mol.* 2018;23(10):2620.
17. Li W, Cheng Z, Wang Y, Qu H. Quality control of *Lonicerae Japonicae* Flos using near infrared spectroscopy and chemometrics. *J Pharm Biomed Anal.* 2013;72:33–9.
18. Wang F, Zhang Z, Cui X, Harrington PB. Identification of rhubarbs by using NIR spectrometry and temperature-constrained cascade correlation networks. *Talanta.* 2006; 70(5):1170–6.
19. Buschmann C. Photoacoustic Spectroscopy and its Application. Vol. 39, Sen'i Gakkaishi. 1983.
20. Teixeira DF, Lucchetti L, Tappin MRR, Cardoso IC, Jacob S. Panorama of quality of Espinheira-Santa samples from local productive arrangements and local stores of Rio De Janeiro assayed by pharmacopoeial methods and principal component analysis. *Rev. Virtual de Química.* 2018;10(1):194–209.
21. Pedroso FB, de Aguiar DBS, de Brito PS, Pessôa CA, Fujiwara ST, Kanunfre CC, et al. Antibacterial and Cytotoxic Activities of Copper-Functionalized Silsesquioxane 3-n-Propylpyridinium Chloride. *Braz Arch Biol Technol.* 2022;65(e22220228):1-10.
22. Gomes MLS, Nascimento NS, Borsato DM, Pretes AP, Nadal JM, Novatski A, et al. Long-lasting anti-platelet activity of cilostazol from poly ( $\epsilon$ -caprolactone)-poly (ethylene glycol) blend nanocapsules. *Mater. Sci. Eng. C.* 2019; 94(31): 694-702.
23. Pupo YM, Farago PV, Nadal JM, Simão LC, Esmerino LA, Gomes OMM, et al. Effect of a novel quaternary ammonium methacrylate polymer (QAMP) on adhesion and antibacterial properties of dental adhesives. *Int. J. Mol. Sci.* 2014;15(5):8998-9015.
24. Tawadare R, Thangadurai D, Khandagave RB, Mundaragi A, Sangeetha J. Phenotypic Characterization and Genetic Diversity of Sugarcane Varieties Cultivated in Northern Karnataka of India based on Principal Component and Cluster Analyses. *Braz Arch Biol Technol.* 2019;62(e19180376):1-12.
25. Nadal JM, dos Anjos GC, Novatski A, Macenhan WR, Dias DT, Barboza FM, et al. Adapalene-loaded poly( $\epsilon$ caprolactone) microparticles: Physicochemical characterization and in vitro penetration by photoacoustic spectroscopy. *PLoS ONE.* 2019;14(3):e0213625:1-20.
26. Grasel FDS, Ferrão MF, Wolf CR. Development of methodology for identification the nature of the polyphenolic extracts by FTIR associated with multivariate analysis. *Spectrochim. Acta A Mol. Biomol. Spectrosc.* 2016;153:94–101.
27. Alves AO, Oliveira RM, Weiss GCC, Bonadiman BSR, Santos RCV. Phytochemical Analysis and Evaluation of Antioxidant and Antimicrobial Activities of *Maytenus Illicifolia*. In: XXV Brazilian Congress of Food Science and Technology, 2016, Gramados. Gramados: FAURGS, 2016.
28. Falcão L, Araújo MEM. Tannins characterisation in new and historic vegetable tanned leathers fibres by spot tests. *J. Cult. Herit.* 2011;12(2):149–56.
29. Falcão L, Araújo MEM. Tannins characterization in historic leathers by complementary analytical techniques ATR-FTIR, UV-Vis and chemical tests. *J. Cult. Herit.* 2013;14(6):499–508.
30. Edelmann A, Lendl B. Toward the optical tongue: Flow-through sensing of tannin– protein interactions based on FTIR spectroscopy. *J. Am. Chem. Soc.* 2002;124(49):14741–7.
31. Arana J, Rendón ET, Rodríguez JMD, Melián JAH, Díaz OG, Peña JP. Highly concentrated phenolic wastewater treatment by the Photo-Fenton reaction, mechanism study by FTIR-ATR. *Chemosphere.* 2001;44(5):1017–1023.
32. Laghi L, Parpinello GP, Del Rio D, Calani L, Mattioli AU, Versari A. Fingerprint of enological tannins by multiple techniques approach. *Food Chem.* 2010;121(3):783–8.

33. Ozgunay H, Sari O, Tozan M. Molecular investigation of valonea tannin. *J. Am. Leather Chem. Assoc.* 2007;102(05):54–157.
34. Fernández K, Agosin E. Quantitative analysis of red wine tannins using Fourier-transform mid-infrared spectrometry. *J. Agric. Food Chem.* 2007;55(18):7294–300.
35. Puică NM, Pui A, Florescu M. FTIR spectroscopy for the analysis of vegetable tanned ancient leather. *Eur. J. Sci. Theol.* 2006;2(4):49–53.
36. Ajuong EM, Redington M. Fourier transform infrared analyses of bog and modern oak wood (*Quercus petraea*) extractives. *Wood Sci. Technol.* 2004;38(3):181–90.
37. Oo C-W, Kassim MJ, Pizzi A. Characterization and performance of *Rhizophora apiculata* mangrove polyflavonoid tannins in the adsorption of copper (II) and lead (II). *Ind. Crops Prod.* 2009;30(1):152–61.
38. Özacar M, Şengil İA, Türkmenler H. Equilibrium and kinetic data, and adsorption mechanism for adsorption of lead onto valonia tannin resin. *Chem. Eng. J.* 2008;143(1–3):32–42.
39. Kim S, Kim HJ. Curing behavior and viscoelastic properties of pine and wattle tannin-based adhesives studied by dynamic mechanical thermal analysis and FT-IR-ATR spectroscopy. *J Adhes Sci Technol.* 2003;17(10):1369–83.
40. Ping L, Pizzi A, Guo ZD, Brosse N. Condensed tannins from grape pomace: characterization by FTIR and MALDI TOF and production of environment friendly wood adhesive. *Ind. Crops Prod.* 2012;40:13–20.
41. Jensen JS, Egebo M, Meyer AS. Identification of spectral regions for the quantification of red wine tannins with Fourier transform mid-infrared spectroscopy. *J. Agric. Food Chem.* 2008;56(10):3493–9.
42. Lazzari E, Schena T, Marcelo MCA, Primaz CT, Silva AN, Ferrão MF, et al. Classification of biomass through their pyrolytic bio-oil composition using FTIR and PCA analysis. *Ind. Crops Prod.* 2018;111(October):856–64.
43. Musa AE, Gasmelseed, GA. Characterization of *Lawsonia inermis* (Henna) as vegetable tanning material. *JFPI* 2012;1(2):35–40.
44. Aslan A. Improving the dyeing properties of vegetable tanned leathers using chitosan formate. *Ekoloji.* 2013;22(86):26–35.
45. Valladão FN, Miranda RRS, Vale FH, Valladão AS, Silva GDF, Duarte LP, et al. Four Brazilian *Maytenus salicifolia* Reissek (Celastraceae) groups studied by TLC and UV/Vis spectrophotometry. *Rev. Bras. Farmacogn.* 2009;19(3):733–9.



© 2023 by the authors. Submitted for possible open access publication under the terms and conditions of the Creative Commons Attribution (CC BY NC) license (<https://creativecommons.org/licenses/by-nc/4.0/>).